

Optimal Design of Pitched Roof Rigid Frames with Non-Prismatic Members Using Quantum Evolutionary Algorithm

Hamed Arzani¹, Ali Kaveh^{2*}, Mohammad Kamalinejad¹

¹ Department of Civil Engineering, Shahid Rajaei Teacher Training University, Tehran Province, Tehran, Lavizan, Iran

² Iran University of Science and Technology, Narmak, Tehran, P.O. Box 16846-13114, Iran

* Corresponding author, e-mail: alikaveh@iust.ac.ir

Received: 27 March 2019, Accepted: 02 April 2019, Published online: 02 May 2019

Abstract

The weight and shape of the gable and multi-span frames (mono and two-span pitched roof) with tapered members, as a familiar group of the pitched roof frames, are highly dependent on the properties of the member cross-section. In this work a quantum inspired evolutionary algorithms, so-called Quantum evolutionary algorithm (QEA) [1], are utilized for optimal design of one gable frame and a multi-span frame in five alternatives with tapered members. In order to optimize the frames, the design is performed using the AISC specifications for stress, displacement and stability constraints. The design constraints and weight of the gable and multi-span frames are computed from the cross-section of members. These optimum weights are obtained using aforementioned optimization algorithm considering the cross-section of members and design constraints as optimization variables and constraints, respectively. A comparative study of the QEA and some recently developed methods from literature is also performed to illustrate the performance of the utilized optimization algorithm and its featuring. Furthermore, optimal design of a multi-span frame is compared with the solution of other methods including the same conditions and constraints. This study indicates the power of QEA in exploring and exploitation due the search space with using Q-gate and binary code for individual representation and updating. Binary code helps the QEA to find optimal solution even with minimum number of Q-bit individuals. High speed of this method is because of such a feature.

Keywords

gable frames, optimal design, meta-heuristic algorithms, tapered members, enhanced quantum inspired evolutionary algorithm, quantum-inspired evolutionary algorithm (QEA)

1 Introduction

Achievement to the least cost and eventually winning the bidding process of a project is pursued as an important goal in a rigorous competition between constructing companies. In this regard, the use of Meta-heuristics optimization algorithms can be a convenient method to achieve this goal. During the price estimation of a project, the weight of structure is very important item because it constitutes 30 % and 40 % of the total cost of the project. In decision-making problem, access to the solution of a certain problem in the least logical possible time is one of the remarkable applications of the metaheuristics optimization algorithms. The slopped roof frames which are widely used in construction of the industrial buildings, gyms, schools and colleges, fire stations, storages, hangars and many other usages are our case study in this paper.

Low rise buildings are including those structures which have mean height less than 18 m [2]. Sloped roof rigid frames are the most common for low-rise buildings, can be categorized based on their shapes, for instance, mono-slope, multi-span, lean to and tee frames and so on. The gable rigid frames are the most used category of this group. Multi-span frames are the second most favorite of this category. These frames may have symmetrical or unsymmetrical geometry.

As it is shown in Figs. 1 and 2, the great number of typical rigid frames in consecutive bays in this kind of buildings enforces the designers to concentrate on minimum weight of frames to achieve the least finishing cost of project. The members of these frames are categorized as prismatic or non-prismatic sections. In non-prismatic



Fig. 1 Perspective layout of a 3D gable frame structure in consecutive bays



Fig. 2 Perspective layout of a 3D two-span frame structure in consecutive bays

type, the cross-section is continuously varying from start to end of linear elements, and in prismatic type, the member has the same geometrical characteristics along the linear element [3, 4].

In the field of structural optimization, there are many research areas and many methods to optimize the cost per weight of structures, such as gradient-based and stochastic optimizers for different structures that are complex [5–7]. Since the 1960s a vast amount of research has been in the area of structural optimization, the majority of which deal with minimizing the weight of the structure. Non-linear mathematical programming is necessary for solving the optimization problems. The main featuring of these methods is robustness that leads to applying them to all types of optimization problems. Several calculations of the objective and constraints function and their derivatives are usually needed when these methods are applied to optimization problems [8]. The last two decades were highlighted by the development and improvement of the metaheuristic methods. Most of them deal with optimal design of two or three dimensional structures such as trusses, frames, dams, etc. [9–13]. A small fraction of the papers published are on real gable frame and saw-tooth structures with tapered members. Therefore, optimal design of the gable rigid frame and saw-tooth with web-tapered members in the low-rise buildings can be an interesting and challenging issue in structural engineering research [14–16].

The main objective of this paper is to find the optimum member sections of a symmetric gable frames and a saw-tooth frame for assessment of QEA. The members of these

frames are also considered as the web-tapered I-section members. The design method used in this study is consistent with ASCE/SEI 7-10 [2] and AISC-LRFD 360-05 Specifications [17].

QEA, quantum evolutionary algorithm, is utilized for finding the optimum weight of frames. QEA belongs to a family of meta-heuristic algorithms which was recently developed by the Han and Kim in 2002 And was inspired quantum mechanics principles in probability states and probability distribution function. In the 1st case study, the obtained results of this new meta-heuristics algorithm have been compared with two recently developed metaheuristic algorithms, namely the Colliding Bodies Optimization (CBO) and Enhanced Colliding Bodies Optimization (ECBO) algorithms [18, 19] and 2nd one indicates the performance of QEA rather than HS (Harmony Search) [20], CBO, ECBO, VPS (Vibrating Particle System) [21] and TLBO (Teaching-Learning Based Optimization) [22]. The ECBO was introduced by Kaveh and Ilchi Ghazaan [19] and it uses memory to save some historically best solution to improve the performance of the CBO.

It should be noted that, since the plan rectilinear shape of gable frame is depended on the dimensions of sections, this work can be considered as the shape optimization of gable frames. In such a gable frame design problem, selecting an appropriate cross-sectional of member is important because it influences the structural analysis and weight of the frames. Therefore, it is often required to find the best set of cross-sections for reducing the weight of gable frames and achieving an optimal and economical design.

The remainder of this paper is organized as follows:

- Explanation of the Quantum evolutionary algorithm is presented in Section 2.
- In Section 3, the mathematical formulations of the structural optimization of the gable rigid frame problems are presented and a brief explanation of the ASCE/SEI 7-10 and AISC-LRFD 360-05 specifications is provided.
- In Section 4 the design examples and the discussions on the results are presented.

2 Quantum evolutionary algorithm

Quantum-inspired evolutionary algorithm (QEA) is recently proposed which can explore the search space with a smaller number of individuals and exploit the search space for a global solution within a short span of time. QEA is based on the concept and principles of quantum computing, such as the quantum hit and the superposition of states.

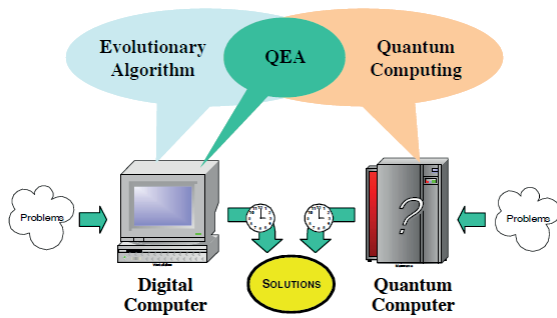


Fig. 3 Quantum-inspired evolutionary algorithm [23]

However, QEA is not a quantum algorithm, but a novel evolutionary algorithm as shown in Fig. 3. Like any other evolutionary algorithms (EAs), QEA is characterized by the representation of the individuals, the evaluation function, and the population dynamics.

QEA was proposed by Han and Kim [1], which was inspired by the concept of quantum computing. In QEA, the smallest unit of information is called a Q-bit, which is defined as $\begin{bmatrix} \alpha \\ \beta \end{bmatrix}$, where α and β are complex numbers that specify the probability amplitudes of the corresponding states. The moduli α^2 and β^2 are the probabilities that the Q-bit exists in state "0" and state "1", respectively, which satisfy $\alpha^2 + \beta^2 = 1$. An m-Q-bits is defined as $\begin{bmatrix} \alpha_1 & \alpha_2 & \dots & \alpha_m \\ \beta_1 & \beta_2 & \dots & \beta_m \end{bmatrix}$ where $|\alpha_j|^2 + |\beta_j|^2 = 1$. ($j = 1, 2, 3 \dots m$) and m is the number of Q-bits.

The procedure of QEA is described as follows:

Procedure of QEA

Begin

Initialize Q(0) at t = 0

Make P(0) by observing the state of Q(0)

Repair P(0)

Evaluate f(X₁⁰)

Store the best solutions among P(0) into B⁰ and f(B⁰)

While (not termination condition) do

Begin

t = t + 1

Make P(t) by observing the state of Q(t)

Repair P(t)

Evaluate f(X₁^t)

Update Q(t) using Q-gate U(t)

Store the best solutions among P(t) into B^t and f(B^t)

End

End

where $Q(t) = \{q_1^t, q_2^t, q_3^t, \dots, q_n^t\}$, $q_i^t = \begin{bmatrix} \alpha_1^t & \alpha_2^t & \alpha_3^t & \dots & \alpha_m^t \\ \beta_1^t & \beta_2^t & \beta_3^t & \dots & \beta_m^t \end{bmatrix}$,

$p(t) = \{X_1^t, X_2^t, X_3^t, \dots, X_n^t\}$, $B^t \in X_j$, $X_1^t = \{x_{11}^t, x_{12}^t, x_{13}^t, \dots, x_{1m}^t\}$
 $i = 1, 2, 3 \dots, n$, $j = 1, 2, 3 \dots, m$, n being the size of the population.

In the step of "Initialize Q(0) at t = 0", $\begin{bmatrix} \alpha_{ij}^0 \\ \beta_{ij}^0 \end{bmatrix}$ of all q_i^0 in Q(0) are initialized with $1/\sqrt{2}$. It means that in each m-Q-bits, q_i^0 represents the linear superposition of all possible states with the same probability.

To obtain the binary string, the step of "Make P(t) by observing the state of Q(t)" can be implemented for each Q-bit individual as follows. When observing the state of, Q(t) the value $x_{ij}^t = 0$ or 1 of P(t) is determined by the probability $|\alpha_{ij}^t|^2$ or $|\beta_{ij}^t|^2$.

Procedure make P(t)

Begin

i = 0

While (i < n) do

i = i + 1

j = 0

While (j < n) do

j = j + 1

If random [0, 1] > $|\alpha_{ij}^t|^2$

Then $x_{ij}^t = 1$

Else $x_{ij}^t = 0$

End

End

End

The steps of "Repair P(t)" and "Evaluate f(X₁^t)" are according to the problems, where f(X) is the fitness function.

The update procedure of Q-bits is introduced as follows:

Procedure update Q(t)

Begin

i = 0

While (i < n) do

i = i + 1

j = 0

While (j < n) do

j = j + 1

Determine $\Delta\theta_{ij}$ with the lookup table

Obtain $\begin{bmatrix} \alpha_{ij}^t \\ \beta_{ij}^t \end{bmatrix}$ as:

$$\begin{bmatrix} \alpha_{ij}^t \\ \beta_{ij}^t \end{bmatrix} = U(t) \begin{bmatrix} \alpha_{ij}^{t-1} \\ \beta_{ij}^{t-1} \end{bmatrix}$$

End

End

End

Quantum gate (Q-gate) U(t) is a variable operator of the QEA. It can be chosen according to the problem. A modified rotation gate used in QEA is as follows:

$$\begin{bmatrix} \alpha'_j \\ \beta'_j \end{bmatrix} = \begin{bmatrix} \cos(\xi(\Delta\theta_j)) & -\sin(\xi(\Delta\theta_j)) \\ \sin(\xi(\Delta\theta_j)) & \cos(\xi(\Delta\theta_j)) \end{bmatrix} \begin{bmatrix} \alpha_j \\ \beta_j \end{bmatrix},$$

where $\xi(\Delta\theta_j) = s(\alpha_j, \beta_j) \times \Delta\theta_j$ and $\Delta\theta_j$ represent the rotation direction and angle, respectively. The lookup table is presented in Table 1. Where delta is the step size and should be designed in compliance with the application problem. However, it has not had the theoretical basis till now, even though it usually is set as small value. In the comparison experiments, we set:

To prevent the premature convergence of Q-bit, gate is defined as a Q-gate extended from the rotation gate:

$$\begin{bmatrix} \alpha'_i \\ \beta'_i \end{bmatrix} = H_\epsilon(\alpha_i, \beta_i, \Delta\theta_i),$$

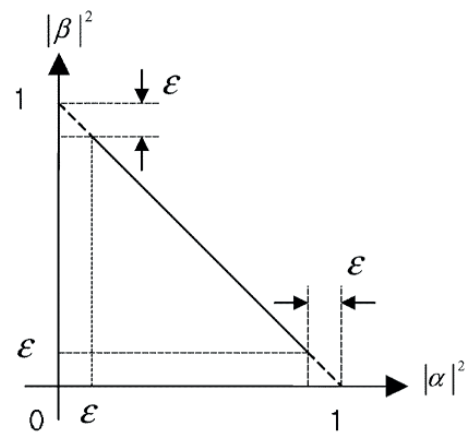
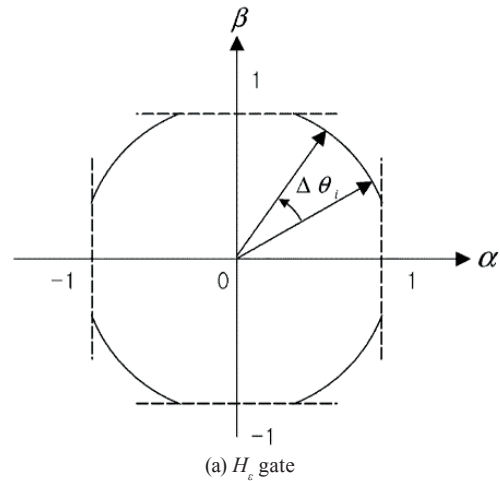
where: $\begin{bmatrix} \alpha''_i \\ \beta''_i \end{bmatrix} = U(\Delta\theta_i) \begin{bmatrix} \alpha'_i \\ \beta'_i \end{bmatrix}$

1. If $|\alpha_i''|^2 \leq \epsilon$ & $|\beta_i''|^2 \geq 1 - \epsilon$ then $\begin{bmatrix} \alpha'_i \\ \beta'_i \end{bmatrix} = \begin{bmatrix} \sqrt{\epsilon} \\ \sqrt{1 - \epsilon} \end{bmatrix}$,
2. If $|\beta_i''|^2 \leq \epsilon$ & $|\alpha_i''|^2 \geq 1 - \epsilon$ then $\begin{bmatrix} \alpha'_i \\ \beta'_i \end{bmatrix} = \begin{bmatrix} \sqrt{\epsilon} \\ \sqrt{1 - \epsilon} \end{bmatrix}$,
3. Else $\begin{bmatrix} \alpha'_i \\ \beta'_i \end{bmatrix} = \begin{bmatrix} \alpha''_i \\ \beta''_i \end{bmatrix}$,

where $0 < \epsilon \ll 1$, $U(\Delta\theta_i)$ is the rotation gate and $\Delta\theta_i, i = 1, 2, \dots, m$, is the rotation angle of each Q-bit toward either 0 or 1 state depending on its sign. Fig. 4 shows the H_ϵ gate and the constraints of where $\lim_{\epsilon \rightarrow 0} H_\epsilon(0)$ is the same as the rotation gate. It should be noted that if ϵ is too big, the convergence tendency of a-bit individual may disappear [23].

3 The rigid frame optimization problems

Many indexes affect the construction cost of the project, the cost of the frames in the gable and multi-span frames design such as wall posts, foundation, purlins, girts, etc. However, the main cost belongs to the structural frames. This cost in turn includes different items such as the frame steel price, and the cutting, fabrication, installation, connections, etc. of the frame. Among all the aforementioned



(b) ϵ constraints.
 Fig. 4 H_ϵ gate based on the rotation gate

Table 1 A modified rotation gate lookup table

x_j	b_j	$f(X) > f(B)$	$\Delta\theta_j$	$s(\alpha_j, \beta_j)$			
				$\alpha_j, \beta_j > 0$	$\alpha_j, \beta_j < 0$	$\alpha_j = 0$	$\beta_j = 0$
0	0	False	0	0	0	0	0
0	0	True	0	0	0	0	0
0	1	False	Delta	+1	-1	0	± 1
0	1	True	Delta	-1	+1	± 1	0
1	0	False	Delta	-1	+1	± 1	0
1	0	True	Delta	+1	-1	0	± 1
1	1	False	0	0	0	0	0
1	1	True	0	0	0	0	0

BUILDING WEIGHT & PRICE SUMMARY		
Description	Total_Wt	Total_Price
Rigid Frames & Endwall Frames	30310.8	28984.3
Door Jambs & Headers	1789.3	1317.4
Purlins, Girts & Eave Struts	18272.7	13243.9
Roof & Wall Sheeting	26289.5	13743.7
Connection Plates	243.9	675.4
Angles	973.8	1482.6
Trim	605.3	179.6
Cables & Sealant	404.4	6386.0
Accessories	6453.6	11774.8
Fasteners	777.1	1699.1
Total:	86120.4	79486.9

Fig. 5 Cost summary sample for a project

items, the most effective parameter is the steel cost that is due to the repetition of a steel frame in consecutive bays. Moreover, the design of foundation and the seismic behavior of structure are significantly dependent upon the weight of the gable frames [24].

The total weight of a steel structure in estimation of its expense has direct interference. This weight includes steel plates, bolts and screws, hot and cold rolled members, steel deck, the weight of the material flowing from the cutting operations to make parts of the steel plate and the weight of the welding material. Fig. 5 shows a sample of cost summary per preliminary estimation for a certain project [25].

The final weight of delivered steel members is greater than the estimated weight when the structure has been designed due to welding material. Regardless of how much the weight of a steel skeleton is at the design stage, cutting methods of steel plates can be effective in increasing or decreasing the finishing weight of consumable materials. The unusable part of steel plates can be decreased by relying on technical drafts obtained from shop drawings and good sort of details on technical drawings for CNC or another cutting methods. Of course the proper management and operator's skill in setting the steel plates pieces on cutting sheet can be efficient on controlling of steel plate wastes. However, difference between weights obtained from shop drawing soft wares such as Tekla structures, MBS (Metal Building Software) and produced members

is not avoidable. In this regard, expert designer uses 3 to 5 percent over-weight for steel built-up members. In the case of hot and cold rolled section elements, the weights of members are used for estimating. In any case, the final cost of the steel structures includes the following:

1. The cost of primary materials includes steel sheets, bolts, hot and cold rolled profiles, panels and decks, fasteners, screws and etc.
2. The cost of cutting, punching and drilling, assembling and welding of parts.
3. The cost of sandblasting and painting the steel members for coating.
4. Shipping cost of made parts to the job site.
5. Installation and crane costs at the site.

In all of these cases, the project costs are based on the obtained weight from the weighbridge. On the other hand, as mentioned above, net weight is determined in the same initial estimate with considering 3-5 percent over-weight for built-up members with good approximation. Therefore, it is possible to carefully optimize the cost of the construction and implementation of steel skeins directly related to design weight. This is why this process is mainly focused on optimizing the weight of the steel skeleton.

Therefore, the weight of rigid frame structures is considered as the objective function in order to reduce the construction cost of the pitched roof frames. The weight of a gable frame structure can be expressed as:

$$W(X) = \sum_{i=1}^n \rho V_i = \sum_{i=1}^n \rho \bar{A}_i l_i, \quad (1)$$

where ρ is weight per volume of steel, V_i and l_i are the volume and length of the i th segment of the rigid frame structure, respectively, \bar{A}_i is the average of starting and ending cross section areas of the i th segment, n is the total number of segments in a gable frame. The exterior penalty function method is employed to transform the constrained optimization problem into an unconstrained one as follows:

$$f_{penalty} = 1 + \gamma_p \sum_{k=1}^K \max(0, g_k(X)), \quad (2)$$

where K is the number of constraints and final objective function will form as below:

$$f_{objective} = f_{penalty} \times W(X). \quad (3)$$

Now the optimization problem can formally be stated as follows:

Find: $X = \{x_1, x_2, \dots, x_m\}$.

To minimize: $f_{objective} = f_{penalty} \times W(X)$.

Subject to: $g_k(X) \leq 0, k = 1, 2, \dots, K$.

And $x_{jmin} \leq x_j \leq x_{jmax}, j = 1, 2, \dots, m$,

where X is the vector of design variables with m unknowns. Also, x_{imin} and x_{imax} are the lower and upper bounds of the design variables vector, respectively.

4 Design constraints

Design constraints are divided into some groups including the deflection, strength and stability constraints. The strength and displacement constraints for steel frames are imposed according to the provisions of LRFD-AISC specification [17]. These constraints are briefly explained in the following:

- Maximum vertical displacement of the pitched roof

$$\frac{\Delta_V}{L} - R_V \leq 0, \quad (4)$$

where Δ_V is the maximum vertical displacement of roof; L is the length of span in the gable frame structure; and R_V is the allowable vertical displacement index which is equal to 1/360 and 1/240 under live and total loading, respectively.

- Maximum horizontal displacement

$$\frac{\Delta_H}{H} - R_H \leq 0 \quad (5)$$

where Δ_H is the maximum horizontal displacement of eaves in the gable frame; H is the eaves height; R_H represents the allowable horizontal displacement index which considered as $H/200$ under the all loadings.

- Strength constraints

$$\left\{ \begin{array}{l} \frac{P_u}{2\phi_c P_n} + \frac{M_u}{\phi_b M_n} - 1 \leq 0, \quad \text{for } \frac{P_u}{\phi_c P_n} < 0.2 \\ \frac{P_u}{\phi_c P_n} + \frac{8M_u}{9\phi_b M_n} - 1 \leq 0, \quad \text{for } \frac{P_u}{\phi_c P_n} \geq 0.2 \end{array} \right\} \quad (6)$$

where P_u is the required strength (tension or compression); P_n is the nominal axial strength (tension or compression); ϕ_c is the resistance factor ($\phi_c = 0.9$ for tension, $\phi_c = 0.85$ for compression); M_u is the required flexural strength; M_n is the nominal flexural strength; and ϕ_b denotes the flexural resistance reduction factor ($\phi_b = 0.90$).

- The buckling constraints

According to the ANSI/AISC 360-05 manual for design of slender compression elements, the reasonable and practical width-to-thickness ratios of $\frac{b_f}{t_f} \leq 18$ and $\frac{h}{t_w} \leq \frac{0.4E}{f_y} \leq 260$ are considered as the constraints for this study. Here, the material characteristics are considered as: $E = 2.1e6$ kg/cm²; $F_y = 2520$ kg/cm² (36 ksi); $\rho = 7850$ kg/m³; and *Poisson's ratio* = 0.3.

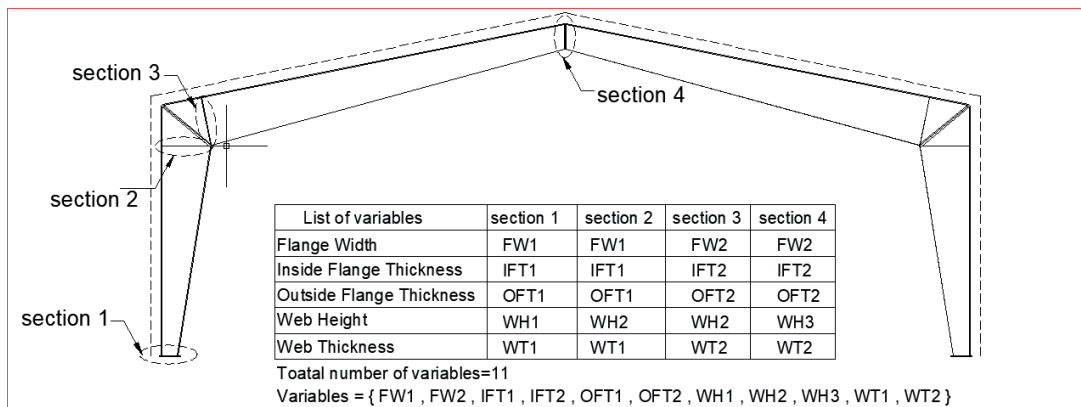


Fig. 6 Definition of considered variables for a pitched gable frame optimization

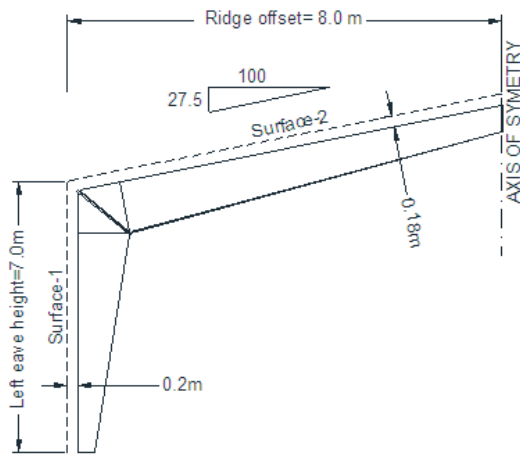


Fig. 7 The frame geometrical layout

• *The stability constraint*

The stability constraints are considered in accordance with the ANSI/ AISC 360-05 manual. In designing the gable frames with web-tapered, achieving the second-order analysis is one of the most significant aspects due to the offset of the cross-section central axis from the chord. This includes the matrix formulations based on the deformed geometry and the *P-delta* analysis procedures [26]. The *P-delta* effects cause the resulting additional force or moment in the members. In this study, the deflection amplification factor, C_d is considered as 4 due to the frame system. Also, the *P-delta* effect is considered on the seismic load combinations.

5 Design Examples

5.1 Pitched Gable Frame (Population number = 30, Max iteration = 100)

In this case, one pitched frame is considered for optimization by QEA, CBO and ECBO algorithms. As appointed in Fig. 6, eleven variables are considered for this case study.

The columns and rafters are web-tapered I-section that may have different inside and outside flange thickness with the same flange width. All geometrical data are shown in Table 2 and the frame geometrical layout is presented in Fig. 7.

The site location had county clay from Kansas in United States of America. As mentioned before, 11 design variables are considered for this case study. In this alternative, the number of Q-bit individuals or agents for these examples is considered 30. The maximum number of iterations is 100. For the sake of simplicity, the penalty approach is used for constraint handling. The optimization algorithms and the analysis and design of structures are coded in Matlab and SAP2000 soft wares, respectively. In the analysis process, a pin-based structural frame is constructed, and the nodal geometry of the members are given based on the neutral axis of the members. An idealized model of a gable frame based on the neutral axis of members is shown in Fig. 8.

Table 2 The geometrical information of the building shape

Geometric parameter	value
Eave height	7.0 m
Slope	27.5 %
Width	16.0 m
Length	18.0 m
Bay spanning	3@6.0 m
Load width of the main frame	6.0 m
Ridge offset	8.0 m
Ridge height	9.2 m
Mean roof height	8.1 m
α = Wall offset in surface 1	0.2 m
β = Roof offset in surfaces 2 and 3	0.18 m
γ = Wall offset in surface 4	0.2 m
Roof slope angle at surface 2	15.37 degree
Roof slope angle at surface 3	15.37 degree

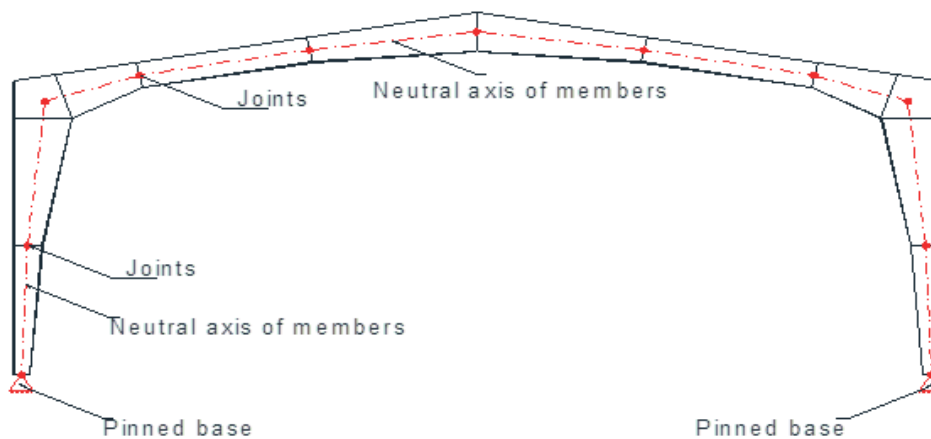


Fig. 8 An idealized model of a gable frame based on the neutral axis of members

For designing the gable frame, two major classes of design variables must be dealt with. The first class is geometric layout variables such as the length of spans or the slope of rafters, the second class is cross section design variables such as dimensions of the starting and ending sections of a segment. In the sizing optimization literature, design variables can be either continuous or discrete. Limitations in the production of various thicknesses of steel sheets give us a limited set of choices. In real applications, the designer is restricted to select the design variables (cross section sizes), from a pre-assigned list of available values [27].

In this example, only the second class of design variables is considered as discrete sizing optimization. These design variables are the dimensions, i.e. the thickness and width of web and flange of cross sections at the intersections of segments of gable frame. In order to make the optimal gable frame model practical, the thickness of webs and flanges should be selected from the discrete set $T = \{0.5, 0.6, 0.8, 1, 1.2, 1.5, 2, 2.5, 3\}$ (cm), the height of webs should be selected from the discrete set $WH = \{15, 20, 25, \dots, 115, 120\}$ (cm), and the width of flanges should be selected from the discrete set $FW = \{15, 20, 25, \dots, 40, 45\}$ (cm). The web thicknesses should be selected equal or less than the flange thicknesses in all member sections for practical application.

Structural Loading

In this study, ASCE/SEI 7-10 (2010) manual is used for considering the dead, live, snow, wind and seismic loads and their influence on the gable frame. The applied loads on the gable rigid frame in low rise buildings generally consist of the vertical and horizontal loads, which are described in the follow subsections.

- *The vertical loads*

In accordance with the ASCE/SEI 7-10 (2010), the most effective vertical loads, which should be considered in the analysis process consist of:

The dead and collateral loads (D)

For considering the dead loads, it is assumed that the type of cladding is a metal sandwich panel with a mass of 14.65 kg/m². This load includes the purlins on the roof and there is no false ceiling. The dead load information is shown in Table 3.

The live loads (L)

According to the ASCE/SEI 7-10 (2010) manual, the live load of a pitched roof is 97.648 kg/m² (20psf), and there is no concentrated load to check the rigid frames with it. It is also assumed that the live load is not reducible. The live load information is shown in Table 4.

Table 3 Summary of the dead loading

Description (unit)	value
Dead load (kg/m ²)	14.64
Load width (m)	6
Uniform dead load (kg/m)	87.84

Table 4 Summary of the live loading

Description (unit)	value
Live load (kg/m ²)	97.648
Load width (m)	6
Uniform live load (kg/m)	585.89

The snow load (SL)

The snow loads consist of the balanced and unbalanced snow loads.

The balanced snow load

The flat roof snow load is evaluated by using the following equation:

$$P_f = 0.7C_e C_t I_s P_g, \tag{7}$$

where the exposure factor, C_e , thermal factor, C_t , and importance factor, I_s , are taken as 1.0 based on sections 7.3.1 through 7.3.3 of ASCE/SEI 7-10 manual. The ground snow load, P_g determined per site-specific analysis is equal to 97.65kg/m² (20.0 psf); thus: $P_f = 14psf$. The snow load acting on a sloping surface are assumed to act on the horizontal projection of that surface. The sloped roof (balanced) snow load, P_s is calculated by multiplying the flat roof snow load, P_f by the roof slope factor, C_s as:

$$P_s = C_s P_f. \tag{8}$$

The roof slope factor, C_s , is taken as 1.0 based on sections 7.4 of ASCE/SEI7-10; thus $p_s = 14.0 psf$ (68.353 kg/m²).

The unbalanced snow loads

According to the ASCE/SEI7-10, for hip and gable roofs with a slope exceeding 7 on 12 (30.2°) or with a slope less than 0.5 on 12 (2.38°) unbalanced snow loads are not required to be applied. Roofs with an eave to ridge distance, W , of less than 6.1 m (20ft) and having simply supported prismatic members, the spanning from ridge to eave should be designed to resist an unbalanced uniform snow load on the leeward side equal to $P_g \times I$. For these roofs the windward side should be unloaded. For all other gable roofs, the unbalanced load should consist of $0.3p_s$ on the windward side, and on the leeward side plus a rectangular surcharge with magnitude $\frac{h_d \gamma}{\sqrt{S}}$ and horizontal extent from the ridge $\frac{8}{3} h_d \sqrt{S}$, where h_d is the drift height (Eq. (13)) which l_u is equal to the eave to ridge distance for the windward portion of the roof, W .

$$h_d = 0.43 \sqrt[3]{I_u} \sqrt[4]{(P_g + 10)} - 1.5 \quad (9)$$

Thus: $p_s = 68.353 \text{ kg/m}^2$, $l_u = 8 \text{ m}$, $P_g = 97.65 \text{ kg/m}^2$, $S = 3.63$, $h_d = 0.45 \text{ m}$.

• *The lateral loads*

In accordance with ASCE/SEI 7-10, the most effective lateral loads, which should be considered in the analysis process, consist of:

The seismic load (E)

The seismic base shear, V , in a given direction is determined according to the following equation:

$$V = C_s W, \quad (10)$$

where C_s and W are the seismic response coefficient and the effective seismic weight, respectively. The seismic response coefficient, C_s , is calculated as:

$$C_s = \frac{S_{DS}}{R I_e} \quad (11)$$

where S_{DS} is the design spectral response acceleration parameter in the short period range, R is the response modification factor and I_e is the importance factor. Because of the location of this case study that is assumed to be at Clay county in Kansas in USA, the mapped Risk-Targeted Maximum Considered Earthquake (MCER) spectral response acceleration parameter for short periods (S_s) and the mapped MCER spectral response acceleration parameter at a period of 1s (S_1) are as 17 % and 5%, respectively. Then, the S_{DS} values are evaluated as 0.2768 and the summarized calculation of the C_s parameter is shown in Table 5.

The wind loads (W)

For evaluating the wind load for a low rise building, the wind pressure is calculated with the following equation:

$$q_z = 0.613 K_z K_{zt} K_d V^2 \left(\frac{N}{m^2} \right); V \text{ in } m/s, \quad (12)$$

where K_d is the wind directionality factor, K_z is the velocity pressure exposure coefficient, K_{zt} is the topographic factor, and V is the basic wind speed. The parameters values used in this study are $K_d = 0.85$, $K_z = 0.93$, $K_{zt} = 1.0$ and $V = 90 \text{ mph}$. In this case study $q_z = 16.365 \text{ psf}$. The velocity pressure at height $h = 26.57 \text{ ft}$, q_h is also taken as 16.876 psf .

The design wind pressures for the frame system of an enclosed and partially enclosed rigid buildings at all heights is determined by the following equation:

$$p = q G C_p - q_i (G C_{pi}), \quad (13)$$

where:

$q = q_z$ for the windward walls evaluated at height z above the ground ($q = 79.90 \text{ kg/m}^2$).

$q = q_h$ for the leeward walls, side walls, and roofs, evaluated at height h ($q = 82.398 \text{ kg/m}^2$).

$q_i = q_h$ for the windward walls, side walls, leeward walls, and roofs of enclosed buildings and for negative internal pressure evaluation in partially enclosed buildings ($q_i = 82.398 \text{ kg/m}^2$).

$q_i = q_z$ for the positive internal pressure evaluation in partially enclosed buildings where height z is defined as the level of the highest opening in the building that could affect the positive internal pressure. For positive internal pressure evaluation, q_i may conservatively be evaluated at height h ($q_i = q_h = 82.398 \text{ kg/m}^2$).

G = gust-effect factor (= 0.85).

p = external pressure coefficient.

$(G C_{pi})$ = internal pressure coefficient $\pm = 0.18$.

Pressure is applied simultaneously on the windward and leeward walls and on the roof surfaces. The coefficient of C_p is defined at two orthogonal directions of wind as shown in Table 6 based on the ASCE 7-10 specification. The values of wind loading on the gable frame are shown in Table 7.

Table 5 The summarized calculation of C_s

Geometric parameter	value
S_{DS}	0.2768
R	4.5
I_e	1
Maximum C_s	0.041
Minimum C_s	0.01
$S_{DS}/R I_e$	0.079
Then $C_s =$	0.041

Table 6 The coefficient of C_p in two orthogonal directions of wind

The directions of wind		C_p
Transvers wind direction (Case 1)	Windward wall	0.8
	Windward roof	-0.7
	Leeward roof	-0.5
	Leeward wall	-0.5
Transvers wind direction (Case 2)	Windward wall	0.8
	Windward roof	-0.18
	Leeward roof	-0.5
	Leeward wall	-0.5

Table 7 The wind load (kg/m) on the gable frame of this study

Surface No.	$GC_{pi} = +0.18$		$GC_{pi} = -0.18$	
	IPP*- Case 1	IPP*- Case 2	IPP*- Case 1	IPP*- Case 2
1	237.02	237.02	415.00	415.00
2	-383.15	-164.63	-205.17	13.35
3	-299.11	-299.11	-121.13	-121.13
4	-288.60	-288.60	-110.62	-110.62

* IPP = Internal positive pressure, INP = Internal negative pressure.

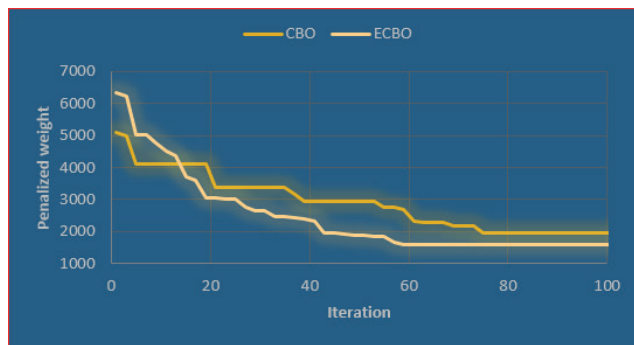


Fig. 9 The convergence history of the best solution with CBO and ECBO



Fig. 10 The convergence history of optimal weight in different iterations of the best solution with QEA (pop. size = 30)

• *Loading combinations*

In this study, basic combinations for strength design are considered based on the ASCE 7-10 manual. The term of $0.2 S_{DS}$ in combinations 5 and 7 is added because of the consideration of vertical seismic load.

1. $1.4 D$
2. $1.2 D + 1.6 L + 0.5(S \text{ or } R)$
3. $1.2 D + 1.6(S \text{ or } R) + (L \text{ or } 0.8 W)$
4. $1.2 D + 1.0 W + L + 0.5(S \text{ or } R)$
5. $(1.2 + 0.2 S_{DS})D + E + L + 0.2 S$
6. $0.9 D + 1.0 W$
7. $(0.9 - 0.2 S_{DS})D + E$

Figs. 9, 10 show the convergence history of the best solutions in different iterations with CBO [16] and QEA. The convergence diagram of the ECBO method is also presented in Fig. 9 [15]. Agent vector and optimal weight of each method have been reported in Table 8.

Discussion and conclusions

Table 8 compares the obtained results from CBO, ECBO and QEA algorithms for this example. As anticipated, the results obtained from QEA are competitive to ECBO and CBO. The weight in QEA method is less than CBO and approximately near to ECBO. In QEA method, achieving to the better solution is possible by increasing the maximum iteration of algorithm up to certain value. One of best characteristic of QEA is related to high pace of algorithm execution. Figs. 9 and 10 show the convergence histories of the best penalized weights obtained using all mentioned algorithms in the optimization process. It can be seen that the optimum weight of the QEA is plunged abruptly in the preliminary iterations and in the remaining of them it is descended tidily. It can be seen from these figures that though the QEA algorithm is considerably faster in the early optimization iterations, the ECBO algorithm converged to a significantly better design in the later optimization iterations

5.2 Two-span frame (Population number = 5, Max iteration = 100)

In the second case study, the frame has two spans, and the number of independent non-prismatic member is five. Fig. 11 shows layout of geometrical information for a two-span frame. These sort of frames are popular in industrial

Table 8 Optimal design of three different algorithms

Algorithm	Surface No.	Element Type	Element No.	Start web height (m)	Flange width (m)	Inside flange thickness (m)	Web thickness (m)	Outside flange thickness (m)	End web height (m)	Weight (kg)
CBO [15]	1	Column	1	0.15	0.2	0.015	0.008	0.01	0.9	1967.3
	2	Beam	2	0.9	0.25	0.01	0.006	0.01	0.35	
ECBO [15]	1	Column	1	0.65	0.2	0.008	0.005	0.008	0.95	1578.4
	2	Beam	2	0.95	0.25	0.008	0.005	0.008	0.3	
QEA (n = 30)	1	Column	1	0.3	0.15	0.015	0.006	0.008	0.9	1694.67
	2	Beam	2	0.9	0.25	0.008	0.006	0.01	0.45	

Table 9 Feasible range of discrete variables

Variable (unit)	Number of variables in agent vector	Feasible value
Tapered length ratio (%)	X1,x2(TLR1, TLR2)	0.1,0.15,0.2,0.25,0.3,0.35,0.4,0.45
Web height (m)	X3,X4,X5,X6,X7,X8,x9	0.4,0.5,0.6,0.7,0.8,0.9,1.0,1.1,1.2
Web thickness (m)	X10	0.008,0.01,0.012
Flange width(m)	-	0.2
Flange thickness (m)	-	0.01

Table 10 Optimum weight of different algorithms for ridge height = 8.1 m

Methods	HS [28]	VPS [28]	CBO [28]	ECBO [28]	TLBO [28]	QEA
Number of population	16	16	16	16	16	5
Maximum Iteration	60	60	60	60	60	102
Optimum weight	3323.48	3324.77	3444.92	3335.2	3305.93	3343.506

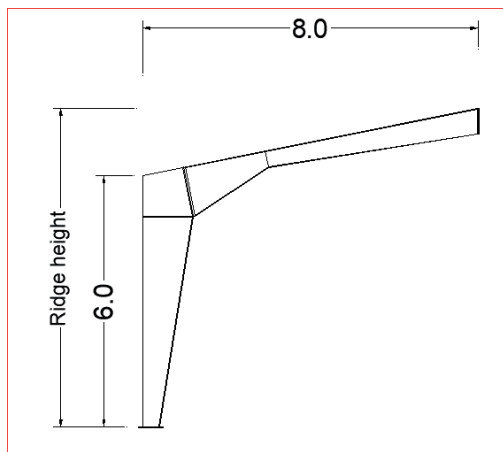


Fig. 11 Geometric parameters of half span in both frames

usages. In this case, the modulus of elasticity of steel and its yield stress is $2.1e6 \text{ kg/cm}^2$ and 2520 kg/cm^2 , respectively. This example focuses on influences of ridge height and slope on weight of two-span frames and the frames with different ridge height and the same length of span are optimized by using QEA method. Results obtained by QEA method are compared with some well-known method such as HS (Harmony Search), TLBO (Teaching-Learning Based Optimization), VPS (Vibrating Particles System), CBO (Colliding Body Optimization) and ECBO (Enhanced Colliding Body Optimization) methods [28]. The effects of frame's ridge height are evaluated on the optimum weight. Minimum and maximum ridge heights are considered as 6.5 m and 8.5 m resulting in 3.58° and 17.35° for the minimum and maximum roof angle, respectively. Frame dimensions and problem variables are shown in Figs. 11 and 12, respectively. The Upper and lower bond for variables is shown in Table 9. Roof gravity distributed loads, including dead, live and snow loads are 480, 576 and 900 kg/cm^2 respectively. Seismic load is considered

as 150 and 100 kg/m uniformly distributed load on the X direction in the rafter and column, respectively. Wind load is considered in accordance with Fig. 13. The optimum weights of the frames with different roof angles are given in Tables 10 and 11. The optimal values for variables for each roof angle are provided in Table 12. The convergence history of optimal weight in different iterations is provided in Figs. 14 to 19. The population size and the number of iterations for all benchmark algorithms are 16 and 60, respectively and for case of this paper are 5 and 102.

Discussion and conclusions

The results of Tables 11 and 12 indicate that the optimized weight of the quantum evolution algorithm is quite competitive with other methods. In some cases, even with a small number of agent population, better weights than those mentioned in the text of this example are obtained, which confirms the power and quality of the quantum evolution algorithm. Apart from the low dependence on the number of agent population, what distinguishes this method from other optimization methods is Heisenberg's uncertainty property, which is an inseparable feature of this algorithm. Figs. 14 to 19 indicate the process of accessing the optimal answer can be continued even after the completion of the maximum number of repetitions, which is an obvious characteristic of evolutionary methods. These methods do not guarantee the absolute optimality of the answers. In fact, according to Heisenberg's principle, at each step of the repetition, we cannot absolutely speak of the accuracy of the optimality of the answers, because in the random and binary generation of solutions, while exploring the entire search space in an appropriate manner and escaping from the local optimal we must expect a solution that is better than what we got before.

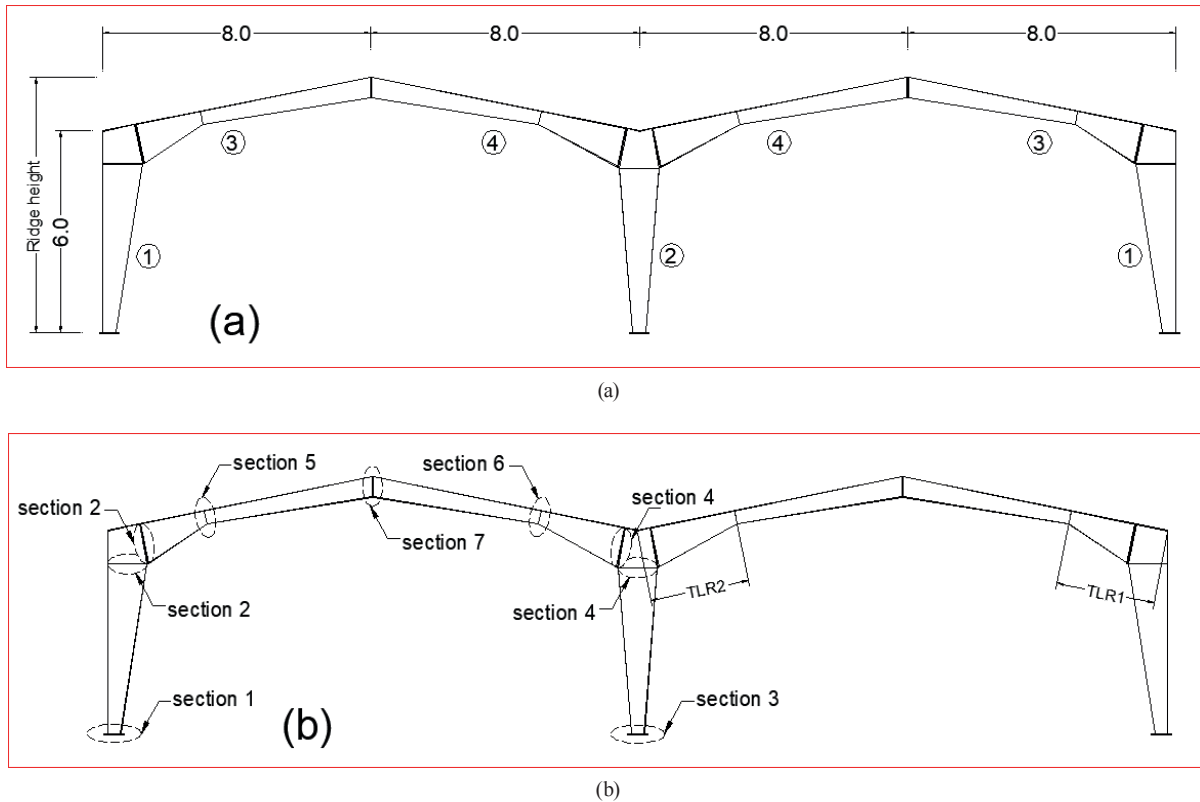


Fig. 12 (a) Element groups of the 2 spans frame. (b) Variables of the 2-span frame

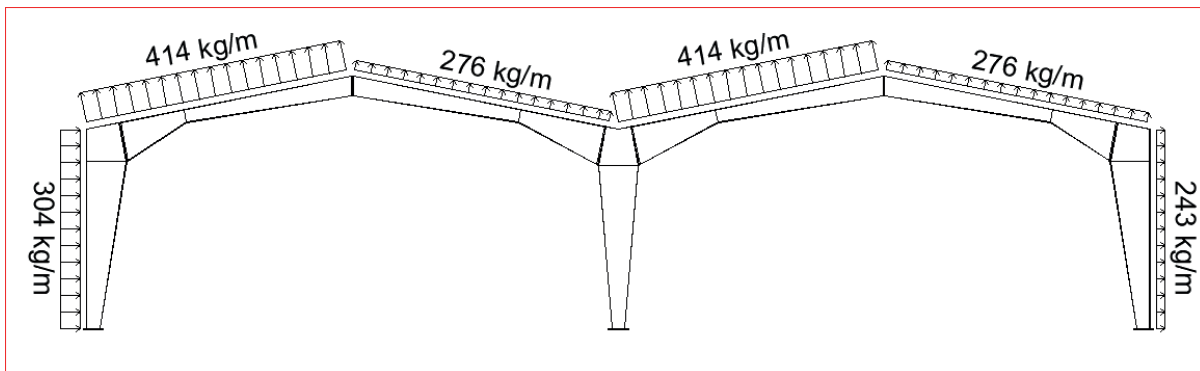


Fig. 13 Wind load on the two-span frame

Table 11 Comparison of obtained optimum weights for different ridge heights and QEA methods

Ridge Ht.	Optimum weight(kg) [28]	QEA (kg)
Ridge Ht. = 6.5	3090.57	2961.079
Ridge Ht. = 6.9	3145.25	3158.558
Ridge Ht. = 7.3	3168.83	3242.604
Ridge Ht. = 7.7	3262.92	3265.919
Ridge Ht. = 8.1	3305.93	3343.506
Ridge Ht. = 8.5	3408.66	3318.529

Table 12 Optimum value of the variables by QEA methods and same work in literature

Methods	Ridge height	X1	X2	X3	X4	X5	X6	X7	X8	X9	X10
Minimum values from HS, TLBO, CBO, ECBO, VPS [28]	6.5	15	40	0.4	0.6	0.4	1	0.4	0.4	0.4	0.008
	6.9	25	30	0.4	0.8	0.4	0.9	0.4	0.4	0.4	0.008
	7.3	20	35	0.4	0.7	0.4	0.9	0.4	0.6	0.4	0.008
	7.7	25	35	0.5	0.8	0.4	1	0.4	0.4	0.4	0.008
	8.1	25	35	0.5	0.8	0.4	1	0.4	0.5	0.4	0.008
	8.5	20	35	0.5	0.8	0.4	0.9	0.4	0.9	0.4	0.008
Minimum values from QEA	6.5	45	25	0.4	1.2	0.4	0.8	0.4	0.4	0.4	0.008
	6.9	35	20	0.4	1.2	1.2	0.7	0.4	0.4	0.6	0.008
	7.3	40	30	0.4	1.1	0.9	0.9	0.4	0.4	0.5	0.008
	7.7	25	35	0.6	1.2	0.6	1	0.4	0.4	0.4	0.008
	8.1	30	25	0.4	1.1	0.4	1.2	0.4	0.4	0.4	0.008
	8.5	30	20	0.4	1.2	0.4	1	0.5	0.4	0.5	0.008



Fig. 14 The convergence history of optimal weight in different iterations with QEA method (pop. size = 5, Ridge Ht. = 6.5 m)



Fig. 17 The convergence history of optimal weight in different iterations with QEA method (pop. size = 5, Ridge Ht. = 7.7 m)

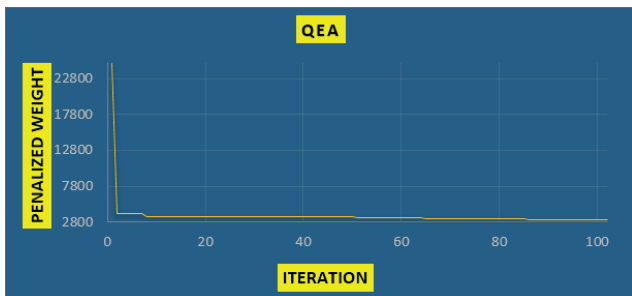


Fig. 15 The convergence history of optimal weight in different iterations with QEA method (pop. size = 5, Ridge Ht. = 6.9 m)



Fig. 18 The convergence history of optimal weight in different iterations with QEA method (pop. size = 5, Ridge Ht. = 8.1 m)



Fig. 16 The convergence history of optimal weight in different iterations with QEA method (pop. size = 5, Ridge Ht. = 7.3 m)



Fig. 19 The convergence history of optimal weight in different iterations with QEA method (pop. size = 5, Ridge Ht. = 8.5 m)

6 Conclusions

To sum up, an efficient optimization method is proposed for optimal design of the symmetric gable frames and a two-span frame with tapered-web I-section members, based on Quantum Evolutionary Algorithm (QEA). The QEA mimics the laws of Quantum mechanics principles. The very simple implementation, parameter independence and binary generation by using Q-gate are definite strength points of QEA. In the QEA, some strategies like different Q-gate have been used to promote the exploitation ability. In order to find the optimal cross section sizes of the frames, the weight of frame and cross section sizes

are respectively defined as the objective function and variables in the optimization process. The cross section sizes are then selected based on optimization algorithms from practical available discrete variables. The validity and efficiency of the proposed method are shown through two examples with different ridge height. The outcomes are that QEA could decrease the weight of the real gable frames without appearing to violate any constraint.

Conflict of interest

On behalf of all authors, the corresponding author states that there is no conflict of interest.

References

- [1] Han, K.-H., Kim, J.-H. "Quantum-inspired evolutionary algorithm for a class of combinatorial optimization", *IEEE Transactions on Evolutionary Computation*, 6(6), pp. 580–593, 2002.
<https://doi.org/10.1109/TEVC.2002.804320>
- [2] ANSI "ASCE/SEI 7-10 Minimum design loads for buildings and other Structures", ASCE, Reston, Virginia, USA, 2015.
- [3] Fraser, D. J. "Design of tapered member portal frames", *Journal of Constructional Steel Research*, 3(3), pp. 20–26, 1983.
[https://doi.org/10.1016/0143-974X\(83\)90003-2](https://doi.org/10.1016/0143-974X(83)90003-2)
- [4] Watwood, V. B. "Gable frame design considerations", *Journal of Structural Engineering*, 111(7), pp. 1543–1558, 1985.
[https://doi.org/10.1061/\(ASCE\)0733-9445\(1985\)111:7\(1543\)](https://doi.org/10.1061/(ASCE)0733-9445(1985)111:7(1543))
- [5] Spires, D., Arora, J. S. "Optimal design of tall RC-framed tube buildings", *Journal of Structural Engineering*, 116(4), pp. 877–897, 1990.
[https://doi.org/10.1061/\(ASCE\)0733-9445\(1990\)116:4\(877\)](https://doi.org/10.1061/(ASCE)0733-9445(1990)116:4(877))
- [6] Saka, M. P., Geem, Z. W. "Mathematical and metaheuristic applications in design optimization of steel frame structures: an extensive review", *Mathematical Problems in Engineering*, 2013.
<https://doi.org/10.1155/2013/271031>
- [7] Kazemizadeh Azad, S., Hasançebi, O. "Discrete sizing optimization of steel trusses under multiple displacement constraints and load cases using guided stochastic search technique", *Structural and Multidisciplinary Optimization*, 52(2), pp. 383–404, 2015.
<https://doi.org/10.1007/s00158-015-1233-0>
- [8] Haftka, R. T., Gurdal, Z. "Element of structural optimization", 3rd ed., Springer, Dordrecht, Netherlands, 1992.
<https://doi.org/10.1007/978-94-011-2550-5>
- [9] Kaveh, A. "Advances in metaheuristic algorithms for optimal design of structures", 2nd ed., Springer International Publishing, Basel, Switzerland, 2017.
<https://doi.org/10.1007/978-3-319-05549-7>
- [10] Saka, M. P. "Optimum design of pitched roof steel frames with haunched rafters by genetic algorithm", *Computers and Structures*, 81(18–19), pp. 1967–1978, 2003.
[https://doi.org/10.1016/S0045-7949\(03\)00216-5](https://doi.org/10.1016/S0045-7949(03)00216-5)
- [11] Tejani, G. G., Bhensdadia, V. H., Bureerat, S. "Examination of three meta-heuristic algorithms for optimal design of planar steel frames", *Advances in Computational Design*, 1(1), pp. 79–86, 2016.
<https://doi.org/10.12989/acd.2016.1.1.079>
- [12] Bhensdadia, V., Tejan, G. "Grey wolf optimizer (GWO) algorithm for minimum weight planer frame design subjected to AISC-LRFD", In: Satapathy S., Joshi A., Modi N., Pathak N. (eds.) *Proceedings of International Conference on ICT for Sustainable Development. Advances in Intelligent Systems and Computing*, 409, Springer, Singapore, 2016, pp. 143–151.
https://doi.org/10.1007/978-981-10-0135-2_13
- [13] Tejani, G. G., Pholdee, N., Bureerat, S., Prayogo, D., Gandomi, A. H. "Structural optimization using multi-objective modified adaptive symbiotic organisms search", *Expert Systems with Applications*, 125, pp. 425–441, 2019.
<https://doi.org/10.1016/j.eswa.2019.01.068>
- [14] Saka, M. P. "Optimum design of steel frames with tapered members", *Computers and Structures*, 63(4), pp. 798–811, 1997.
[https://doi.org/10.1016/S0045-7949\(96\)00074-0](https://doi.org/10.1016/S0045-7949(96)00074-0)
- [15] Kaveh, A., Mahdavi, V. R., Kamalinejad, M. "Optimal design of the monopole structures using CBO and ECBO algorithms", *Periodica Polytechnica Civil Engineering*, 61(1), pp. 110–116, 2017.
<https://doi.org/10.3311/PPci.8546>
- [16] Kaveh, A., Ghafari, M. H. "Geometry and sizing optimization of steel pitched roof frames with tapered members using nine meta-heuristics", *Iranian Journal of Science and Technology, Transactions of Civil Engineering*, 43(1), pp. 1–8, 2019.
<https://doi.org/10.1007/s40996-018-0132-1>
- [17] "ANSI/AISC 360-05 Specification for structural steel buildings", Chicago, Illinois, USA, 2005.
- [18] Kaveh, A., Mahdavi, V. R. "Colliding bodies optimization: extensions and applications", 1st ed., Springer, Basel, Switzerland, 2015.
<https://doi.org/10.1007/978-3-319-19659-6>
- [19] Kaveh, A., Ilchi Ghazaan, M. "Enhanced colliding bodies optimization for design problems with continuous and discrete variables", *Advances in Engineering Software*, 77, pp. 66–75, 2014.
<https://doi.org/10.1016/j.advengsoft.2014.08.003>
- [20] Geem, Z. W., Kim, J. H., Loganathan, G. V. "A new heuristic optimization algorithm: harmony search", *Simulation*, 76(2), pp. 60–68, 2001.
<https://doi.org/10.1177/003754970107600201>
- [21] Kaveh, A., Ilchi Ghazaan, M. "Vibrating particles system algorithm for truss optimization with multiple natural frequency constraints", *Acta Mechanica*, 228(1), pp. 307–322, 2017.
<https://doi.org/10.1007/s00707-016-1725-z>

- [22] Toğan, V. "Design of planar steel frames using teaching–learning based optimization", *Engineering Structures*, 34, pp. 225–232, 2012. <https://doi.org/10.1016/j.engstruct.2011.08.035>
- [23] Han, K.-H., Kim, J.-H. "Quantum-inspired evolutionary algorithms with a new termination criterion, H/sub /spl epsi// gate, and two-phase scheme", *IEEE Transactions on Evolutionary Computation*, 8(2), pp. 156–169, 2004. <https://doi.org/10.1109/TEVC.2004.823467>
- [24] Hwang, J.-S., Chang, K.-C., Lee, G. C. "Seismic behavior of gable frame consisting of tapered members", *Journal of Structural Engineering*, 117(3), pp. 808–821, 1991. [https://doi.org/10.1061/\(ASCE\)0733-9445\(1991\)117:3\(808\)](https://doi.org/10.1061/(ASCE)0733-9445(1991)117:3(808))
- [25] MBS, "Metal Building Software", [software] Available at: <http://www.mbsweb.com> [Accessed: 29.04.2019]
- [26] Saffari, H., Rahgozar, R., Jahanshahi, R. "An efficient method for computation of effective length factor of columns in a steel gabled frame with tapered members", *Journal of Constructional Steel Research*, 64(4), pp. 400–406, 2008. <https://doi.org/10.1016/j.jcsr.2007.09.001>
- [27] Kazemizadeh Azad, S., Hasançebi, O. "Computationally efficient discrete sizing of steel frames via guided stochastic search heuristic", *Computers and Structures*, 156, pp. 12–28, 2015. <https://doi.org/10.1016/j.compstruc.2015.04.009>
- [28] Kaveh, A., Kabir, M. Z., Bohlool, M. "Optimal design of multi-span pitched roof frames with tapered members", *Periodica Polytechnica Civil Engineering*, 63(1), pp. 77–86, 2019. <https://doi.org/10.3311/PPci.13107>